

EPJ manuscript No.
(will be inserted by the editor)

Study of multi-muon events produced in $p\bar{p}$ interactions at $\sqrt{s} = 1.96$ TeV

T. Aaltonen²², J. Adelman¹², B. Álvarez González¹⁰, S. Amerio^{40,41}, D. Amidei³³, A. Anastassov³⁶, J. Antos¹³, G. Apollinari¹⁶, A. Apresyan⁴⁸, T. Arisawa⁵⁴, A. Artikov¹⁴, W. Ashmanskas¹⁶, P. Azzurri^{43,46}, W. Badgett¹⁶, B.A. Barnett²⁴, V. Bartsch³⁰, D. Beecher³⁰, S. Behari²⁴, G. Bellettini^{43,44}, D. Benjamin¹⁵, D. Bisello^{40,41}, I. Bizjak^{30,l}, C. Blocker⁷, B. Blumenfeld²⁴, A. Bocci¹⁵, V. Boisvert⁴⁹, G. Bolla⁴⁸, D. Bortoletto⁴⁸, J. Boudreau⁴⁷, A. Bridgeman²³, L. Brigliadori⁴⁰, C. Bromberg³⁴, E. Brubaker¹², J. Budagov¹⁴, H.S. Budd⁴⁹, S. Budd²³, S. Burke¹⁶, K. Burkett¹⁶, G. Busetto^{40,41}, P. Bussey^{20,e}, K. L. Byrum², S. Cabrera^{15,k}, C. Calancha³¹, M. Campanelli³⁴, F. Canelli¹⁶, B. Carls²³, R. Carosi⁴³, S. Carrillo^{17,g}, B. Casal¹⁰, M. Casarsa¹⁶, A. Castro^{5,6}, P. Catastini^{43,45}, D. Cauz^{51,52}, V. Cavaliere^{43,45}, S.H. Chang^{25,26,27,28,29}, Y.C. Chen¹, M. Chertok⁸, G. Chiarelli⁴³, G. Chlachidze¹⁶, K. Cho^{25,26,27,28,29}, D. Chokheli¹⁴, J.P. Chou²¹, K. Chung¹¹, Y.S. Chung⁴⁹, C.I. Ciobanu⁴², M.A. Ciocci^{43,45}, A. Clark¹⁹, D. Clark⁷, G. Compostella⁴⁰, M.E. Convery¹⁶, J. Conway⁸, M. Cordelli¹⁸, G. Cortiana^{40,41}, C.A. Cox⁸, D.J. Cox⁸, F. Crescioli^{43,44}, C. Cuenca Almenar^{8,k}, J. Cuevas^{10,j}, J.C. Cully³³, D. Dagenhart¹⁶, M. Datta¹⁶, T. Davies²⁰, P. de Barbaro⁴⁹, M. Dell'Orso^{43,44}, L. Demortier⁵⁰, J. Deng¹⁵, M. Deninno⁵, G.P. di Giovanni⁴², B. Di Ruzza^{51,52}, J.R. Dittmann⁴, S. Donati^{43,44}, J. Donini⁴⁰, T. Dorigo⁴⁰, J. Efron³⁷, R. Erbacher⁸, D. Errede²³, S. Errede²³, R. Eusebi¹⁶, W.T. Fedorko¹², J.P. Fernandez³¹, R. Field¹⁷, G. Flanagan⁴⁸, R. Forrest⁸, M.J. Frank⁴, M. Franklin²¹, J.C. Freeman¹⁶, I. Furic¹⁷, M. Gallinaro⁵⁰, J. Galyardt¹¹, F. Garbersen⁹, J.E. Garcia¹⁹, A.F. Garfinkel⁴⁸, K. Genser¹⁶, H. Gerberich²³, D. Gerdes³³, V. Giakoumopoulou³, P. Giannetti⁴³, K. Gibson⁴⁷, J.L. Gimmell⁴⁹, C.M. Ginsburg¹⁶, N. Giokaris³, M. Giordani^{51,52}, P. Giromini¹⁸, G. Giurgiu²⁴, V. Glagolev¹⁴, D. Glenzinski¹⁶, N. Goldschmidt¹⁷, A. Golossanov¹⁶, G. Gomez¹⁰, M. Goncharov³², O. González³¹, I. Gorelov²¹, A.T. Goshaw¹⁵, K. Goulianos⁵⁰, A. Gresele^{40,41}, S. Grinstein²¹, J. Guimaraes da Costa²¹, Z. Gunay-Unalan³⁴, K. Hahn³², S.R. Hahn¹⁶, B.-Y. Han⁴⁹, J.Y. Han⁴⁹, F. Happacher¹⁸, M. Hare⁵³, R.M. Harris¹⁶, M. Hartz⁴⁷, K. Hatakeyama⁵⁰, S. Hewamanage⁴, D. Hidas¹⁵, C.S. Hill^{9,b}, A. Hocker¹⁶, S. Hou¹, R.E. Hughes³⁷, J. Huston³⁴, J. Incandela⁹, A. Ivanov⁸, E.J. Jeon^{25,26,27,28,29}, M.K. Jha⁵, S. Jindariani¹⁶, W. Johnson⁸, M. Jones⁴⁸, K.K. Joo^{25,26,27,28,29}, S.Y. Jun¹¹, J.E. Jung^{25,26,27,28,29}, D. Kar¹⁷, Y. Kato³⁹, B. Kilminster¹⁶, D.H. Kim^{25,26,27,28,29}, H.S. Kim^{25,26,27,28,29}, H.W. Kim^{25,26,27,28,29}, J.E. Kim^{25,26,27,28,29}, M.J. Kim¹⁸, S.B. Kim^{25,26,27,28,29}, Y.K. Kim¹², L. Kirsch⁷, S. Klimentov¹⁷, B. Knuteson³², B.R. Ko¹⁵, D.J. Kong^{25,26,27,28,29}, J. Konigsberg¹⁷, A. Korytov¹⁷, D. Krop¹², N. Krumnack⁴, M. Kruse¹⁵, V. Krutelyov⁹, N.P. Kulkarni⁵⁵, Y. Kusakabe⁵⁴, S. Kwang¹², A.T. Laasanen⁴⁸, S. Lami⁴³, R.L. Lander⁸, K. Lannon^{37,i}, G. Latino^{43,45}, I. Lazzizzera^{40,41}, H.S. Lee¹², S. Leone⁴³, M. Lindgren¹⁶, A. Lister⁸, D.O. Litvintsev¹⁶, M. Loreti^{40,41}, L. Lovas¹³, D. Lucchesi^{40,41}, P. Lukens¹⁶, G. Lungu⁵⁰, R. Lysak¹³, R. Madrak¹⁶, K. Maeshima¹⁶, K. Makhoul³², T. Maki²², P. Maksimovic²⁴, A. Manousakis-Katsikakis³, F. Margaroli⁴⁸, C.P. Marino²³, V. Martin^{20,f}, R. Martínez-Ballarín³¹, M. Mathis²⁴, P. Mazzanti⁵, P. Mehtala²², P. Merkel⁴⁸, C. Mesropian⁵⁰, T. Miao¹⁶, N. Miladinovic⁷, R. Miller³⁴, C. Mills²¹, A. Mitra¹, G. Mitselmakher¹⁷, N. Moggi⁵, C.S. Moon^{25,26,27,28,29}, R. Moore¹⁶, A. Mukherjee¹⁶, R. Mumford²⁴, M. Mussini^{5,6}, J. Nachtman¹⁶, I. Nakano³⁸, A. Napier⁵³, V. Necula¹⁵, O. Norniella²³, E. Nurse³⁰, S.H. Oh¹⁵, Y.D. Oh^{25,26,27,28,29}, I. Oksuzian¹⁷, T. Okusawa³⁹, R. Orava²², S. Pagan Griso^{40,41}, E. Palencia¹⁶, V. Papadimitriou¹⁶, A.A. Paramonov¹², B. Parks³⁷, G. Pauletta^{51,52}, M. Paulini¹¹, D.E. Pellett⁸, A. Penzo⁵¹, T.J. Phillips¹⁵, G. Piacentino⁴³, L. Pina¹⁷, K. Pitts²³, O. Poukhov^{14,†}, F. Prakoshyn¹⁴, A. Pronko¹⁶, F. Ptohos^{16,d}, E. Pueschel¹¹, A. Rahaman⁴⁷, N. Ranjan⁴⁸, I. Redondo³¹, V. Rekovic³⁵, F. Rimondi^{5,6}, A. Robson²⁰, T. Rodrigo¹⁰, E. Rogers²³, S. Rolli⁵³, R. Roser¹⁶, M. Rossi⁵¹, R. Rossin⁹, A. Ruiz¹⁰, J. Russ¹¹, V. Rusu¹⁶, W.K. Sakumoto⁴⁹, L. Santi^{51,52}, K. Sato¹⁶, A. Savoy-Navarro⁴², P. Schlabach¹⁶, E.E. Schmidt¹⁶, M.A. Schmidt¹², M. Schmitt³⁶, T. Schwarz⁸, L. Scodellaro¹⁰, A. Sedov⁴⁸, S. Seidel³⁵, Y. Seiya³⁹, A. Semenov¹⁴, L. Sexton-Kennedy¹⁶, F. Sforza⁴³, A. Sfyrla²³, S.Z. Shalhout⁵⁵, S. Shiraiishi¹², M. Shochet¹², A. Sidoti⁴³, A. Sisakyan¹⁴, A.J. Slaughter¹⁶, J. Slaunwhite³⁷, K. Sliwa⁵³, J.R. Smith⁸, A. Soha⁸, V. Sorin³⁴, P. Squillacioti^{43,45}, R. St. Denis²⁰, D. Stentz³⁶, J. Strologas³⁵, G.L. Strycker³³, J.S. Suh^{25,26,27,28,29}, A. Sukhanov¹⁷, I. Suslov¹⁴, R. Takashima³⁸, R. Tanaka³⁸, M. Tecchio³³, P.K. Teng¹, K. Terashi⁵⁰, J. Thom^{16,c}, A.S. Thompson²⁰, G.A. Thompson²³, P. Ttito-Guzmán³¹, S. Tokar¹³, K. Tollefson³⁴, S. Torre¹⁸, D. Torretta¹⁶, P. Totaro^{51,52}, S. Tourneur⁴², M. Trovato⁴³, S.-Y. Tsai¹, S. Vallecorsa¹⁹, N. van Remortel^{22,a}, A. Varganov³³, E. Vataga^{43,46}, F. Vázquez^{17,g}, G. Velev¹⁶, C. Vellidis³, V. Veszpremi⁴⁸, M. Vidal³¹, R. Vidal¹⁶, I. Vila¹⁰, R. Vilar¹⁰, T. Vine³⁰, M. Vogel³⁵, G. Volpi^{43,44}, R.G. Wagner², R.L. Wagner¹⁶, T. Wakisaka³⁹, S.M. Wang¹, B. Whitehouse⁵³, E. Wicklund¹⁶, S. Wilbur¹², P. Wittich^{16,c}, S. Wolbers¹⁶, C. Wolfe¹², T. Wright³³, X. Wu¹⁹, K. Yamamoto³⁹, U.K. Yang^{12,h}, Y.C. Yang^{25,26,27,28,29}, K. Yorita¹², T. Yoshida³⁹, G.B. Yu⁴⁹, I. Yu^{25,26,27,28,29}, S.S. Yu¹⁶, J.C. Yun¹⁶,

A. Zanetti⁵¹, X. Zhang²³, S. Zucchelli^{5,6},

(CDF Collaboration)

- ¹ Institute of Physics, Academia Sinica, Taipei, Taiwan 11529, Republic of China
 - ² Argonne National Laboratory, Argonne, Illinois 60439, USA
 - ³ University of Athens, 157 71 Athens, Greece
 - ⁴ Baylor University, Waco, Texas 76798, USA
 - ⁵ Istituto Nazionale di Fisica Nucleare Bologna, I-40127 Bologna, Italy
 - ⁶ Istituto Nazionale di Fisica Nucleare Bologna, ^wUniversity of Bologna, I-40127 Bologna, Italy
 - ⁷ Brandeis University, Waltham, Massachusetts 02254, USA
 - ⁸ University of California, Davis, Davis, California 95616, USA
 - ⁹ University of California, Santa Barbara, Santa Barbara, California 93106, USA
 - ¹⁰ Instituto de Fisica de Cantabria, CSIC-University of Cantabria, 39005 Santander, Spain
 - ¹¹ Carnegie Mellon University, Pittsburgh, PA 15213, USA
 - ¹² Enrico Fermi Institute, University of Chicago, Chicago, Illinois 60637, USA
 - ¹³ Comenius University, 842 48 Bratislava, Slovakia; Institute of Experimental Physics, 040 01 Kosice, Slovakia
 - ¹⁴ Joint Institute for Nuclear Research, RU-141980 Dubna, Russia
 - ¹⁵ Duke University, Durham, North Carolina 27708, USA
 - ¹⁶ Fermi National Accelerator Laboratory, Batavia, Illinois 60510, USA
 - ¹⁷ University of Florida, Gainesville, Florida 32611, USA
 - ¹⁸ Laboratori Nazionali di Frascati, Istituto Nazionale di Fisica Nucleare, I-00044 Frascati, Italy
 - ¹⁹ University of Geneva, CH-1211 Geneva 4, Switzerland
 - ²⁰ Glasgow University, Glasgow G12 8QQ, United Kingdom
 - ²¹ Harvard University, Cambridge, Massachusetts 02138, USA
 - ²² Division of High Energy Physics, Department of Physics, University of Helsinki and Helsinki Institute of Physics, FIN-00014, Helsinki, Finland
 - ²³ University of Illinois, Urbana, Illinois 61801, USA
 - ²⁴ The Johns Hopkins University, Baltimore, Maryland 21218, USA
 - ²⁵ Center for High Energy Physics: Kyungpook National University, Daegu 702-701, Korea
 - ²⁶ Seoul National University, Seoul 151-742, Korea
 - ²⁷ Sungkyunkwan University, Suwon 440-746, Korea
 - ²⁸ Korea Institute of Science and Technology Information, Daejeon, 305-806, Korea
 - ²⁹ Chonnam National University, Gwangju, 500-757, Korea
 - ³⁰ University College London, London WC1E 6BT, United Kingdom
 - ³¹ Centro de Investigaciones Energeticas Medioambientales y Tecnologicas, E-28040 Madrid, Spain
 - ³² Massachusetts Institute of Technology, Cambridge, Massachusetts 02139, USA
 - ³³ University of Michigan, Ann Arbor, Michigan 48109, USA
 - ³⁴ Michigan State University, East Lansing, Michigan 48824, USA
 - ³⁵ University of New Mexico, Albuquerque, New Mexico 87131, USA
 - ³⁶ Northwestern University, Evanston, Illinois 60208, USA
 - ³⁷ The Ohio State University, Columbus, Ohio 43210, USA
 - ³⁸ Okayama University, Okayama 700-8530, Japan
 - ³⁹ Osaka City University, Osaka 588, Japan
 - ⁴⁰ Istituto Nazionale di Fisica Nucleare, Sezione di Padova-Trento, I-35131 Padova, Italy
 - ⁴¹ Istituto Nazionale di Fisica Nucleare, University of Padova, I-35131 Padova, Italy
 - ⁴² LPNHE, Universite Pierre et Marie Curie/IN2P3-CNRS, UMR7585, Paris, F-75252 France
 - ⁴³ Istituto Nazionale di Fisica Nucleare Pisa, I-56127 Pisa, Italy
 - ⁴⁴ Istituto Nazionale di Fisica Nucleare Pisa, University of Pisa, I-56127 Pisa, Italy
 - ⁴⁵ Istituto Nazionale di Fisica Nucleare Pisa, University of Siena, I-56127 Pisa, Italy
 - ⁴⁶ Istituto Nazionale di Fisica Nucleare Pisa, Scuola Normale Superiore, I-56127 Pisa, Italy
 - ⁴⁷ University of Pittsburgh, Pittsburgh, Pennsylvania 15260, USA
 - ⁴⁸ Purdue University, West Lafayette, Indiana 47907, USA
 - ⁴⁹ University of Rochester, Rochester, New York 14627, USA
 - ⁵⁰ The Rockefeller University, New York, New York 10021, USA
 - ⁵¹ Istituto Nazionale di Fisica Nucleare Trieste/Udine, 34100 Trieste, Italy
 - ⁵² University of Trieste/Udine, 33100 Udine, Italy
 - ⁵³ Tufts University, Medford, Massachusetts 02155, USA
 - ⁵⁴ Waseda University, Tokyo 169, Japan
 - ⁵⁵ Wayne State University, Detroit, Michigan 48201, USA
-

the date of receipt and acceptance should be inserted later

Abstract. We report the results of a study of multi-muon events produced at the Fermilab Tevatron collider and acquired with the CDF II detector using a dedicated dimuon trigger. The production cross section and kinematics of events in which both muon candidates are produced inside the beam pipe of radius 1.5 cm are successfully modeled by known processes which include heavy flavor production. In contrast, we are presently unable to fully account for the number and properties of the remaining events, in which at least one muon candidate is produced outside of the beam pipe, in terms of the same understanding of the CDF II detector, trigger, and event reconstruction.

[†] Deceased

^a Visitor from Universiteit Antwerpen, B-2610 Antwerp, Belgium

^b Visitor from University of Bristol, Bristol BS8 1TL, United Kingdom

^c Visitor from Cornell University, Ithaca, NY 14853, USA

^d Visitor from University of Cyprus, Nicosia CY-1678, Cyprus

^e Visitor from Royal Society of Edinburgh/Scottish Executive Support Research Fellow

^f Visitor from University of Edinburgh, Edinburgh EH9 3JZ, United Kingdom

^g Visitor from Universidad Iberoamericana, Mexico D.F., Mexico

^h Visitor from University of Manchester, Manchester M13 9PL, England

ⁱ Visitor from University of Notre Dame, Notre Dame, IN 46556, USA

^j Visitor from University de Oviedo, E-33007 Oviedo, Spain

^k Visitor from IFIC(CSIC-Universitat de Valencia), 46071 Valencia, Spain

^l On leave from J. Stefan Institute, Ljubljana, Slovenia

This Letter summarizes the findings of a study of multi-muon production in $p\bar{p}$ interactions at $\sqrt{s} = 1.96$ TeV [1]. The investigation was motivated by the presence of several inconsistencies that affect or affected the $b\bar{b}$ production at the Tevatron: (a) the ratio of the observed $b\bar{b}$ correlated production cross section to the next-to-leading-order QCD prediction is 1.15 ± 0.21 when b quarks are selected via secondary vertex identification, whereas this ratio is found to be significantly larger than two when identifying b quarks through their semileptonic decays [2]; (b) sequential semileptonic decays of single b quarks are supposedly the main source of dileptons with invariant mass smaller than that of a b quark, but the observed dimuon invariant mass spectrum is not well modeled by the simulation of this process [3]; and (c) the value of $\bar{\chi}$, the average time integrated mixing probability of b flavored hadrons derived from the ratio of muon pairs from b and \bar{b} quarks semileptonic decays with same and opposite sign charge, is measured at hadron colliders to be larger than that measured by the LEP experiments [4,5].

This analysis follows and complements a recent study [6] by the CDF collaboration which has used a dimuon data sample to re-measure the correlated $\sigma_{b \rightarrow \mu, \bar{b} \rightarrow \mu}$ cross section. We use the same data and Monte Carlo simulated samples, and the same analysis methods. The data sample is defined by events containing two central ($|\eta| < 0.7$) muons, each with transverse momentum $p_T \geq 3$ GeV/ c , and with invariant mass larger than 5 GeV/ c^2 . The determination of the data sample composition relies upon the high precision charged particle tracking provided by the CDF II detector [7]. Accurate track impact parameter [8] and primary event vertex determinations are provided by a large central drift chamber surrounding a trio of silicon tracking devices collectively referred to in this letter as the ‘‘SVX’’. The SVX is composed of eight layers of silicon microstrip detectors ranging in radius from 1.5 to 28 cm in the pseudorapidity region $|\eta| < 1$.

In Ref. [6], the value of $\sigma_{b \rightarrow \mu, \bar{b} \rightarrow \mu}$ is determined by fitting the impact parameter distribution of these primary muons with the expected shapes from all sources believed to be significant: semileptonic heavy flavor decays, prompt quarkonia decays, Drell-Yan production, and instrumental backgrounds from prompt hadrons or hadrons from heavy flavor decays which mimic a muon signal [9]. In the following, the sum of these processes will be referred to as the prompt plus heavy flavor (P+HF) contribution to the dimuon sample.

To ensure an accurate impact parameter measurement, analyses performed by the CDF collaboration customarily require that each muon track is reconstructed using silicon hits in at least three out of the eight SVX layers (referred to as standard SVX selection in the following). However, in order to properly model the data with the templates of the various P+HF sources, the study in Ref. [6] has used stricter selection criteria, referred to as tight SVX selection in the following, by requiring muon tracks with hits in the two innermost layers of the SVX detector, and at least in two of the next four outer layers. The size of each P+HF source in the data sample is evaluated by dividing the event yield returned by the fit by the corresponding efficiency of the tight SVX selection, and will later be extrapolated to a sample selected with standard SVX criteria in order to compare with previous measurements. Using control samples of data from various sources ($J/\psi \rightarrow \mu^+\mu^-$, $B^\pm \rightarrow \mu^+\mu^-K^\pm$, $B \rightarrow \mu D^0$, and $\Upsilon \rightarrow \mu^+\mu^-$) we measure the efficiency of the tight SVX selection to be 0.257 ± 0.004 for prompt dimuons and 0.237 ± 0.001 for dimuons produced by heavy flavor decays.

Using the fit result and the above mentioned efficiencies, Reference [6] reports $\sigma_{b \rightarrow \mu, \bar{b} \rightarrow \mu} = 1549 \pm 133$ pb for muons with $p_T \geq 3$ GeV/ c and $|\eta| \leq 0.7$. That result is in good agreement with theoretical expectations as well as with analogous measurements that identify b quarks via secondary vertex identification [10,11]. However, it is also substantially smaller than previous measurements of this cross section [12,13], and raises some concerns about the traditional understanding of the composition of the initial dimuon sample prior to the tight SVX requirements. Based on the sample composition determined by the fit to the muon impact parameter distribution, we expect that $(24.4 \pm 0.2)\%$ of the initial sample should pass the tight SVX selection. However, the fraction of dimuon events in the initial sample that survive the tight SVX selection is significantly smaller $(19.30 \pm 0.04)\%$.

The tight SVX requirements used in Ref. [6] select events in which both muons arise from parent particles that have decayed within a distance of $\simeq 1.5$ cm from the $p\bar{p}$ interaction primary vertex in the plane transverse to the beamline. Using Monte Carlo generated samples of events that are passed through the CDF detector simulation, we estimate that approximately 96% of the dimuon events due to P+HF processes satisfy this condition. Therefore, the fact that the observed efficiency for the tight SVX requirements (19.3%) is significantly smaller than the expected one (24.4%) suggests the additional presence of an important source of dimuons produced beyond 1.5 cm which is suppressed by the tight SVX requirements. Because unnoticed by previous experiments, we whimsically refer to this source of dimuons as the ghost contribution.

The size of the ghost contribution is evaluated as the difference between the total number of dimuon events, prior to any SVX requirements, and the P+HF contribution estimated as the number of events surviving the tight SVX requirements divided by the efficiency of the tight SVX selection [14]. In a data sample corresponding to an integrated luminosity of 742 pb $^{-1}$, 143743 dimuon events survive the tight SVX cuts [15]. After dividing by the 24.4% efficiency, 589111 ± 4829 events are expected in the initial dimuon sample, whereas 743006 are observed. The difference, 153895 ± 4829 events, which is the source of the efficiency discrepancy described above, is comparable in magnitude to the expected dimuon contribution from $b\bar{b}$ production, 221564 ± 11615 events [6].

The standard SVX selection accepts muons from parent particles with decay lengths as long as 10.6 cm. The standard SVX selection reduces the size of the ghost contribution by a factor of two, whereas 88% of the P+HF contribution survives. Table 1 summarizes the sample composition of the dimuon sample for the different SVX selections. In this table and throughout this Letter, the P+HF contribution is estimated from the sample of dimuons surviving the tight SVX requirements and properly accounting for the relevant SVX efficiencies using the sample composition determined by the impact parameter fits of Ref. [6]. The ghost contribution will always be estimated from the total number of observed events after subtracting the P+HF contribution. Since the tight SVX sample is well modeled by fits only using prompt and heavy flavor contributions [6], it seems reasonable to start with the assumption that the ghost contribution in that sample is negligible (set to zero in Table 1). In order to later discuss the effect of ghost events on the $\bar{\chi}$ measurements at hadron colliders, we also provide event yields separately for the subset of events in which the dimuons have opposite-sign (*OS*) and same-sign (*SS*) charge. The ratio of *OS* to *SS* dimuons is approximately 2:1 for P+HF processes and 1:1 for ghost events.

Table 1. Number of events that pass different SVX requirements. Dimuons are also split into pairs with opposite (*OS*) and same (*SS*) sign charge.

Selection	No SVX	Tight SVX	Standard SVX
Total	743006	143743	590970
Total <i>OS</i>		98218	392020
Total <i>SS</i>		45525	198950
P+HF	589111 ± 4829	143743	518417 ± 7264
P+HF <i>OS</i>		98218	354228 ± 4963
P+HF <i>SS</i>		45525	164188 ± 2301
Ghost	153895 ± 4829	0	72553 ± 7264
Ghost <i>OS</i>		0	37792 ± 4963
Ghost <i>SS</i>		0	34762 ± 2301

Thus far, by varying the SVX selection requirements, we have identified a previously ignored contribution to the dimuon triggered sample. The relative size of this contribution depends upon the type of SVX requirement applied to the trigger muons. As the SVX requirements select trigger muons produced closer to the beamline, the size of the ghost contribution is reduced in comparison to that of the P+HF components that are not strongly affected by this requirement. In the following, we describe some of the properties of the ghost contribution followed by a discussion of possible sources. We then discuss how ghost events provide a plausible explanation to the inconsistencies in $b\bar{b}$ production and decay outlined at the beginning of this Letter.

The general nature of ghost events can be characterized by four main features:

- The impact parameter distribution of the trigger muons is significantly different than that of the P+HF contribution.
- In small angular cones around the trigger muons the rate of additional muons is significantly higher than that expected for P+HF processes.
- The distribution of the invariant mass of pairs of trigger and additional muons looks different from that expected from sequential semileptonic decays of hadrons with heavy flavor.
- The impact parameter distribution of the additional muons has the same shape as that of primary muons.

We now briefly describe each of these features. Additional detail on all of the studies outlined below may be found in Ref. [1].

Figure 1 shows impact parameter distributions of trigger muons selected with standard SVX requirements in P+HF and ghost events. The average impact parameter of ghost muons is significantly larger than that of muons due to P+HF production. It follows that, when fitting a dimuon sample containing ghost events with impact parameter templates for muons due to prompt, *c*-quark, and *b*-quark production, the ghost contribution is attributed by the fit to *b*-quark production, the component with the longest lifetime. Therefore, the measured *b*-quark production cross section is augmented by the ratio of ghost to $b\bar{b}$ events in that sample which in turns depends on the SVX selection criteria applied to the trigger muons.

We have studied the rate and kinematics of additional muons with $p_T \geq 2$ GeV/*c* and $|\eta| \leq 1.1$ produced around each primary muon to verify if the inconsistency reported in Ref. [3] is also related to the presence of ghost events. According to the simulation [1], additional muons arise from sequential decays of single *b* hadrons. In addition, one expects a contribution due to hadrons mimicking the muon signal. To account for the fake muon contribution, we apply to all candidate tracks a parametrized probability of penetrating the calorimeter and producing fake muons. This probability has been measured using pions and kaons from decays of D^* mesons [1,6]. This procedure provides

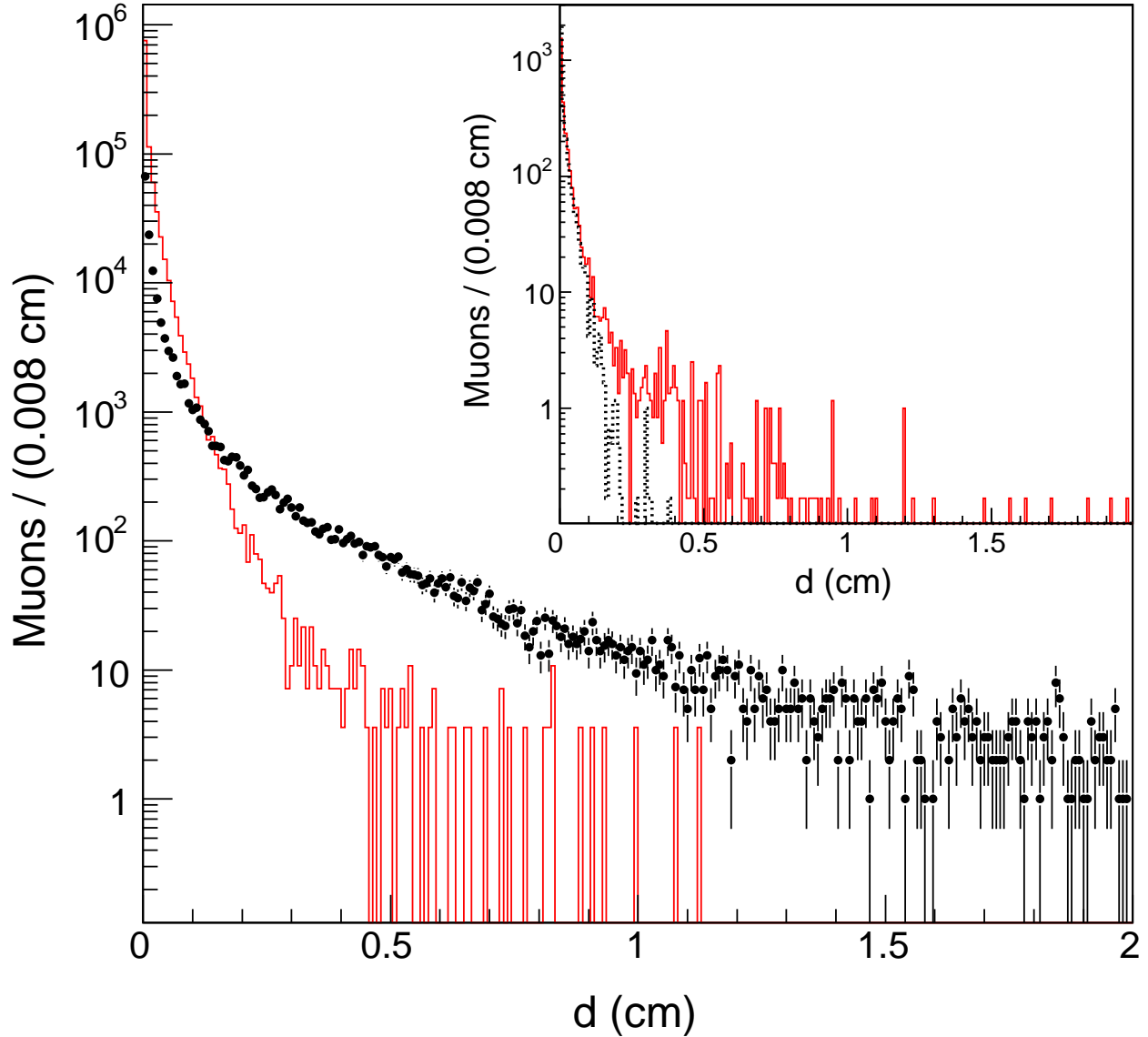


Fig. 1. Impact parameter distribution of muons due to the ghost (\bullet) and P+HF (histogram) contributions. Muon tracks are selected with standard SVX requirements. The detector resolution is $\simeq 30 \mu\text{m}$, whereas bins are $80 \mu\text{m}$ wide. In the insert, we show the same distribution (histogram) for simulated muons that pass the same analysis selection as the data and arise from the in-flight-decays of pions and kaons produced in a heavy flavor simulation (the dotted histogram shows the impact parameter of the parent hadrons).

a detector and kinematic acceptance five times larger than that for trigger muons at the price of a tenfold increase of the fake rate. Since additional muons are searched for offline and there are no trigger rate constraints, this method is the one customarily used by CDF analyses to tag semileptonic decays of heavy flavors [3,10,16]. In the following, muon yields corrected for the fake contribution are referred to as real muons.

Requesting the presence of at least one muon in addition to the two primary (trigger) muons modifies the sample composition relative to the initial sample and is expected to significantly enhance the $b\bar{b}$ contribution. After correcting for fake muons, we expect $b\bar{b}$ production to dominate the sample with three or more muons. The contribution of events without heavy flavor is suppressed by the request of an additional muon. For example, in events containing an $\Upsilon(1S)$ candidate that are included in the dimuon sample, the probability of finding an additional muon is $(0.90 \pm 0.01)\%$.

In the data, 9.7% of the dimuon events contain an additional muon (71835 out of 743006 events). When comparing the efficiency of the tight SVX requirements applied to the primary muon pair, we observe the efficiency to drop from $(19.30 \pm 0.04)\%$ for the full sample to $(16.6 \pm 0.1)\%$ in the subsample that contains at least one additional muon. The drop of the SVX efficiency is a direct indication that ghost events are a larger fraction of the sample containing at least one additional muon. In the original dimuon sample, the ghost contribution accounts for $(20.9 \pm 0.8)\%$ of the sample prior to any SVX requirements. When we request an additional muon, the ghost contribution accounts for $(32.0 \pm 0.7)\%$ of the sample. In other words, ghost events contain more additional muons than the P+HF contribution.

Next, we summarize a detailed study of the rate and kinematic properties of events that contain at least one additional muon. In this measurement, we use the full data sample of 1426 pb^{-1} corresponding to 1426571 events. The full 1426 pb^{-1} data sample consists of 1131090 ± 9271 P+HF events and 295481 ± 9271 ghost events. Each additional muon is combined with the closest primary muon. Combinations of primary and additional muons in ghost events are observed to have smaller opening angles than muon pairs from sequential semileptonic b -decays [1]. Therefore, the study of the ghost sample is further restricted to muons and tracks contained in a cone of angle $\theta \leq 36.8^\circ$ ($\cos \theta \geq 0.8$) around the direction of each primary muon. The number of additional muons contained in these angular cones is listed in Table 2. As reported in Ref. [1], less than half of the OS and SS muon combinations in the ghost sample can be accounted for by fake muons. After removing the fake muon contribution, the rate of additional real muons per event $(9.4 \pm 0.2)\%$ in the ghost sample is four times larger than in the P+HF sample $(2.16 \pm 0.05)\%$. Reference [1] investigates at length the possibility that the predicted rate of fake muons is underestimated. For example, the fourfold increase of the rate of additional real muons per event is verified by selecting additional muons with $p_T \geq 3 \text{ GeV}/c$ and $|\eta| \leq 0.7$. The muon detector and kinematic acceptance is reduced by a factor of five, but, because of the larger number of interaction lengths traversed by hadronic tracks, the contribution of fake muons is negligible [6]. In this case, the rate of additional real muons per event increases from $(0.40 \pm 0.01)\%$ in the P+HF sample to $(1.64 \pm 0.08)\%$ in the ghost sample.

Table 2. Numbers of additional muons with an angle $\theta \leq 36.8^\circ$ with respect to the direction of one of the primary muons. We list separately the combination of additional and primary muons with opposite (OS) and same (SS) sign charge.

Topology	Total	P+HF	Ghost
OS	83237	54545 ± 447	28692 ± 447
SS	50233	30053 ± 246	20180 ± 246

In contrast with the P+HF sample, which contains no more than one real OS additional muon from sequential semileptonic decays of single b quarks and in which SS combinations are accounted for by the predicted rate of fake muons, the ghost sample contains both SS and OS additional real muons. Figure 2 shows the multiplicity distribution of additional muons in ghost events.

As shown in Fig. 3, when applying the tight SVX criteria to primary muons, the invariant mass spectrum of opposite-charge pairs of primary and additional muons is well described by the simulation which is dominated by sequential semileptonic decays of single b quarks. In this case, we observe 6935 ± 154 events, whereas 6918 ± 293 are predicted. In contrast, without any SVX requirement the invariant mass spectrum cannot be modeled with the simulation (37042 ± 389 events are observed and 28589 ± 1213 events are predicted) and the inconsistencies at low invariant mass reported in [3] are reproduced. However, the number of J/ψ mesons in the data is correctly modeled by the simulation in which events containing a J/ψ meson recoiling against another primary muon only arise from $b\bar{b}$ production. This agreement for events in which the trigger muons are selected with no SVX requirements supports the estimate of the tight SVX selection efficiency and the resulting value of $\sigma_{b \rightarrow \mu, \bar{b} \rightarrow \mu}$ reported in Ref. [6].

For the ghost sample, Figure 4 shows the two-dimensional distribution of the impact parameter of a primary muon versus that of all additional muons in a $\cos \theta \geq 0.8$ cone around its direction. The impact parameter distribution of the additional muons is quite similar to that of primary muons even if additional muons are not required to originate at a distance larger than 1.5 cm from the beamline. However, the impact parameters of the additional and primary muons are loosely correlated (the correlation factor is approximately 0.03) [17].

We use samples of data not contaminated by ghost events to verify that large muon impact parameters are not a detector artifact. As shown in Fig. 5, when primary muons are accompanied by a reconstructed $D^0 \rightarrow \pi^+ K^-$ decay, the impact parameter distributions are exhausted beyond 0.5 cm. As shown in Fig. 6, the impact parameter distribution of additional real muons is exhausted beyond 0.5 cm if the primary muons are selected with tight SVX criteria. As shown in Fig. 7, the same is true for additional muons selected as in this analysis and accompanying a $D^0 \rightarrow \pi^+ K^-$ candidate that triggered the event acquisition [18]. In conclusion, the shape of the muon impact parameter distribution in ghost events is not caused by poor detector resolution or pattern recognition errors in the event reconstruction.

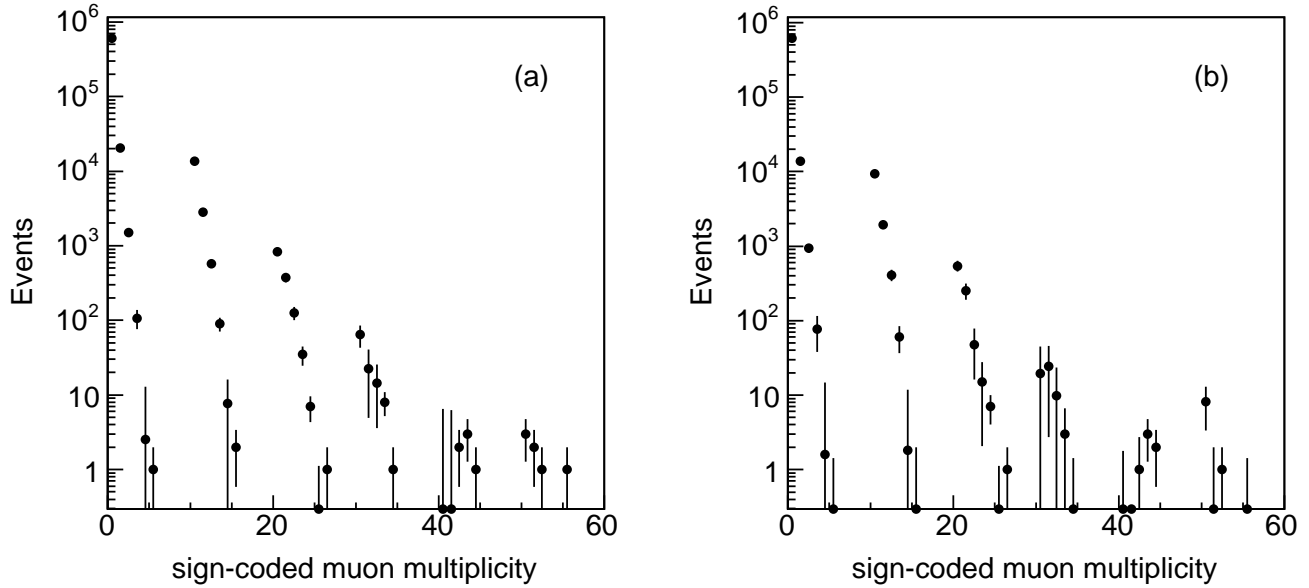


Fig. 2. Multiplicity distribution of additional muons found in a $\cos \theta \geq 0.8$ cone around the direction of a primary muon in the ghost sample before (a) and after (b) correcting for the fake muon contribution. An additional muon increases the multiplicity by 1 when it has opposite and by 10 when it has same sign charge as the primary muon. The first bin indicates events without additional muons.

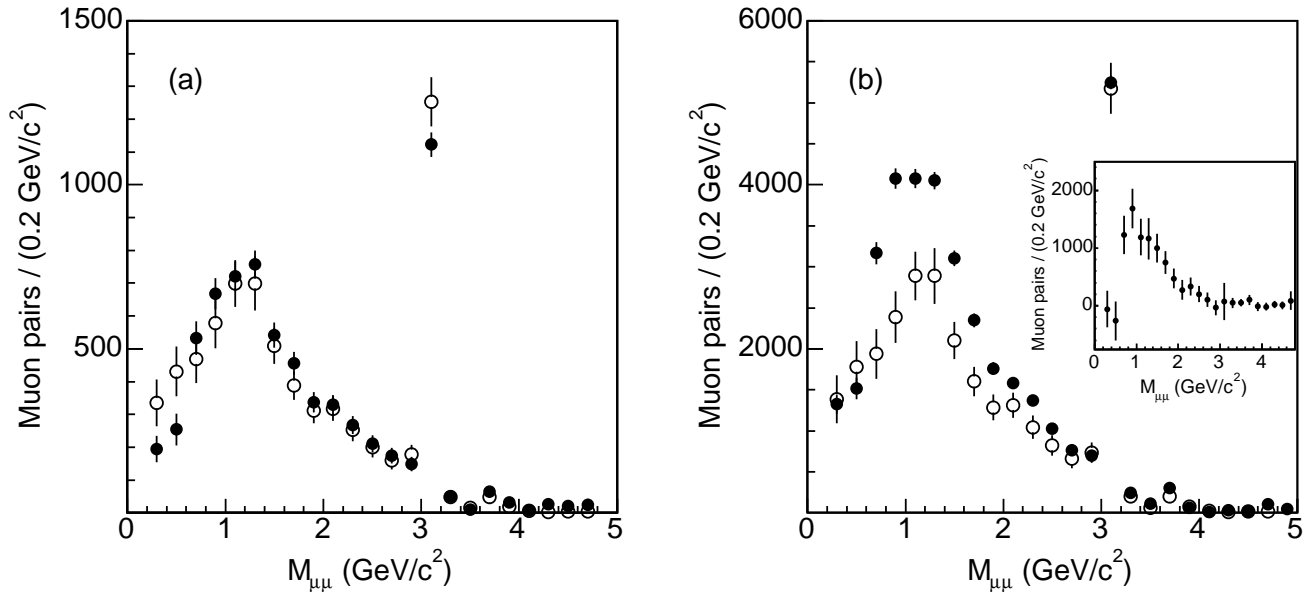


Fig. 3. The invariant mass distribution of opposite-charge muon pairs in the data (\bullet) is compared to the simulation prediction (\circ) for primary muons selected with (a) tight or (b) no SVX requirements. One of the two primary muons in the event is combined with an additional muon of opposite charge if their invariant mass is smaller than $5 \text{ GeV}/c^2$. The fake muon contribution has been accounted for. The simulation prediction uses the measured $\sigma_{b \rightarrow \mu, \bar{b} \rightarrow \mu}$ and $\sigma_{c \rightarrow \mu, \bar{c} \rightarrow \mu}$ cross sections [6] and the same luminosity of the data. The insert shows the difference between data and prediction.

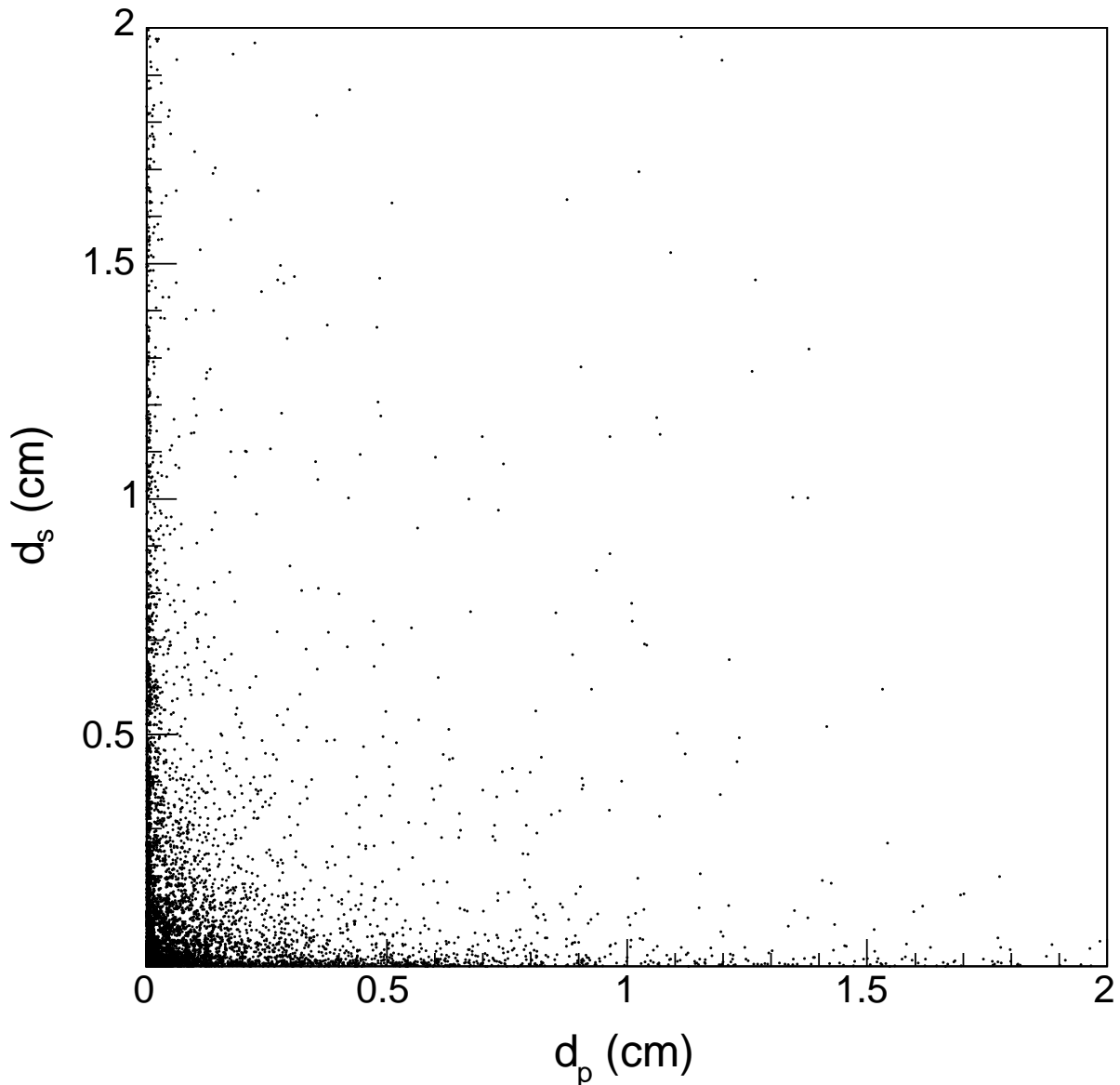


Fig. 4. Two-dimensional distribution of the impact parameter of a primary muon, d_p , versus that, d_s , of additional muons in the ghost sample. All muons are selected with standard SVX requirements.

The impact parameter distributions of all additional muons in the dimuon sample are shown in Fig. 8. The P+HF contribution does not produce additional muons with impact parameters larger than 0.5 cm. Fits with an exponential function to the impact parameter distributions of additional muons in the range 0.5 – 2.0 cm where no heavy flavor contribution is expected, return a slope of approximately 21.4 ± 0.5 ps. Non-triggering prongs of K_S^0 decays reconstructed in the dimuon data set are the analogous of additional muons. As demonstrated in Ref. [1], fits to the distribution of their impact parameters with values larger than 0.5 cm return the correct K_S^0 lifetime. If the observed impact parameter tail in Fig. 8 were due to known particles with lifetime longer than heavy flavor - such as pions, kaons, K_S^0 , and hyperons - one would have observed a slope at least as large as 90 ps.

We have considered a number of potential sources that could produce muons with impact parameter much larger than what it is expected from heavy flavor decays. The one source found to contribute significantly arises from in-flight-decays of pions and kaons. Based upon a generic QCD simulation, we predict a contribution of 57000 events [1], 44% and 8% of which pass the loose and tight SVX selection, respectively. The uncertainty of this prediction is difficult

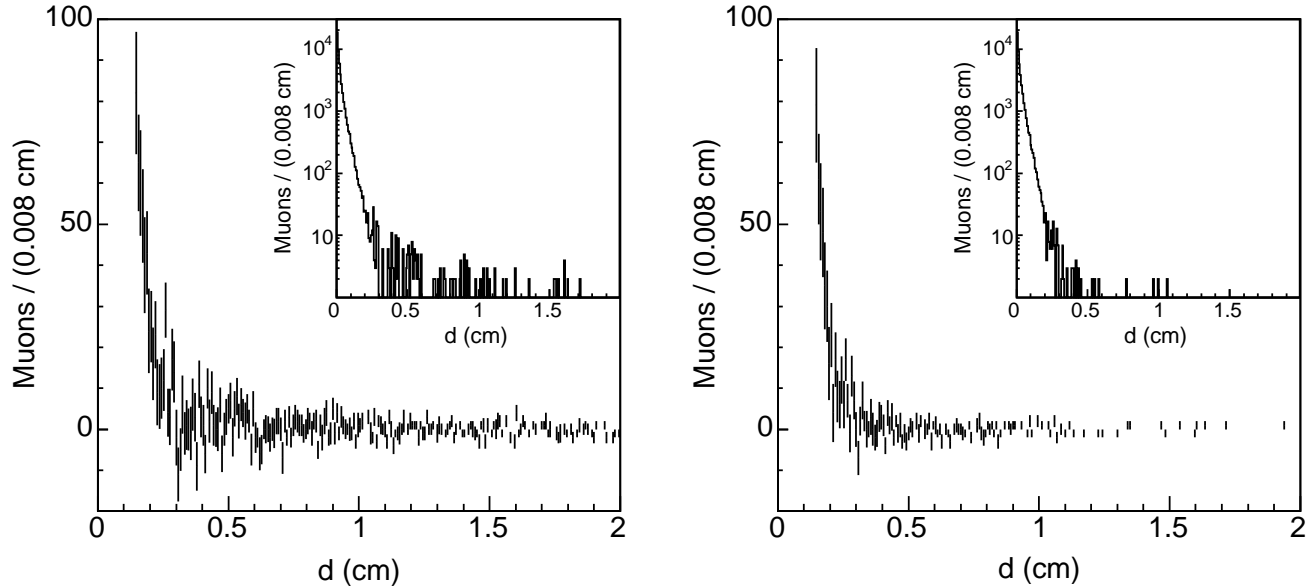


Fig. 5. Magnified views of the impact parameter distribution of primary muons that are accompanied by a reconstructed $D^0 \rightarrow \pi^+ K^-$ decay. The insert shows the entire distribution. Muons are selected with (left) no or (right) standard SVX requirements. The combinatorial background under the D^0 signal has been removed with a sideband subtraction method.

to assess, but, as shown by the insert in Fig. 1, in-flight decays alone cannot account for the shape of the muon impact parameter distribution in the ghost sample. A smaller contribution ($\simeq 12000$ events) from K_S^0 and hyperon decays in which the punchthrough of a hadronic prong mimics a muon signal is estimated using the data. Secondary inelastic interactions in the tracking volume and cosmic rays are found to be a negligible source of ghost events. Our estimate of the size of possible sources of ghost events underpredicts the observed number by approximately a factor of two (154000 observed and 69000 accounted for). While this difference is not significant because of a possibly large uncertainty in the in-flight-decay prediction, in-flight-decays cannot account for ghost events with a muon multiplicity higher than that of events due to heavy flavor production. Since ghost events were originally identified as a subsample suppressed by the tight SVX requirement, we have now identified a puzzling correlation between primary muons originating from decay vertices more displaced than those of heavy flavors and the muon multiplicity in these events.

Taken as a whole, it seems difficult to reconcile the rates and characteristics of the ghost events with expectations from known sources. A large portion of these events is certainly due to muons arising from in-flight-decays of pions and kaons or punchthrough of hadronic prongs of K_S^0 and hyperon decays. However, a small but significant fraction of these events has features that cannot be explained with our present understanding of the CDF II detector, trigger and event reconstruction.

Although we cannot fully explain the composition of the ghost sample in terms of known sources, the identification of this type of event provides a plausible resolution to the set of inconsistencies mentioned at the beginning of this Letter. The general observation is that the measured $\sigma_{b \rightarrow \mu, \bar{b} \rightarrow \mu}$ increases as the trigger muons are allowed to originate at increasing distances from the primary event vertex, and is almost a factor of two larger than that measured in [6] when no distance requirement is made [13]. As mentioned above, the magnitude of the ghost contribution is comparable to the $b\bar{b}$ contribution when no SVX selection is made and in combination would account for the measurement reported in [13]. Similarly, for the standard SVX criteria, the magnitude of the ghost contribution (72553 ± 7264 events, equally split in OS and SS dimuons), when added to the $b\bar{b}$ contribution of 194976 ± 10221 events [6], coincides with the cross section measurement reported in [12] and the $\bar{\chi}$ value reported in [4] since these measurements use similar sets of SVX requirements. Finally, the ghost sample is now understood to be the source of the dimuon invariant mass discrepancy observed in Ref. [3].

We thank the Fermilab staff and the technical staffs of the participating institutions for their vital contributions. This work was supported by the U.S. Department of Energy and National Science Foundation; the Italian Istituto Nazionale di Fisica Nucleare; the Ministry of Education, Culture, Sports, Science and Technology of Japan; the National Science Council of the Republic of China; the Swiss National Science Foundation; the A.P. Sloan Foundation; the Korean Science and Engineering Foundation and the Korean Research Foundation; the Particle Physics and Astronomy Research Council and the Royal Society, UK; the Institut National de Physique Nucleaire et Physique

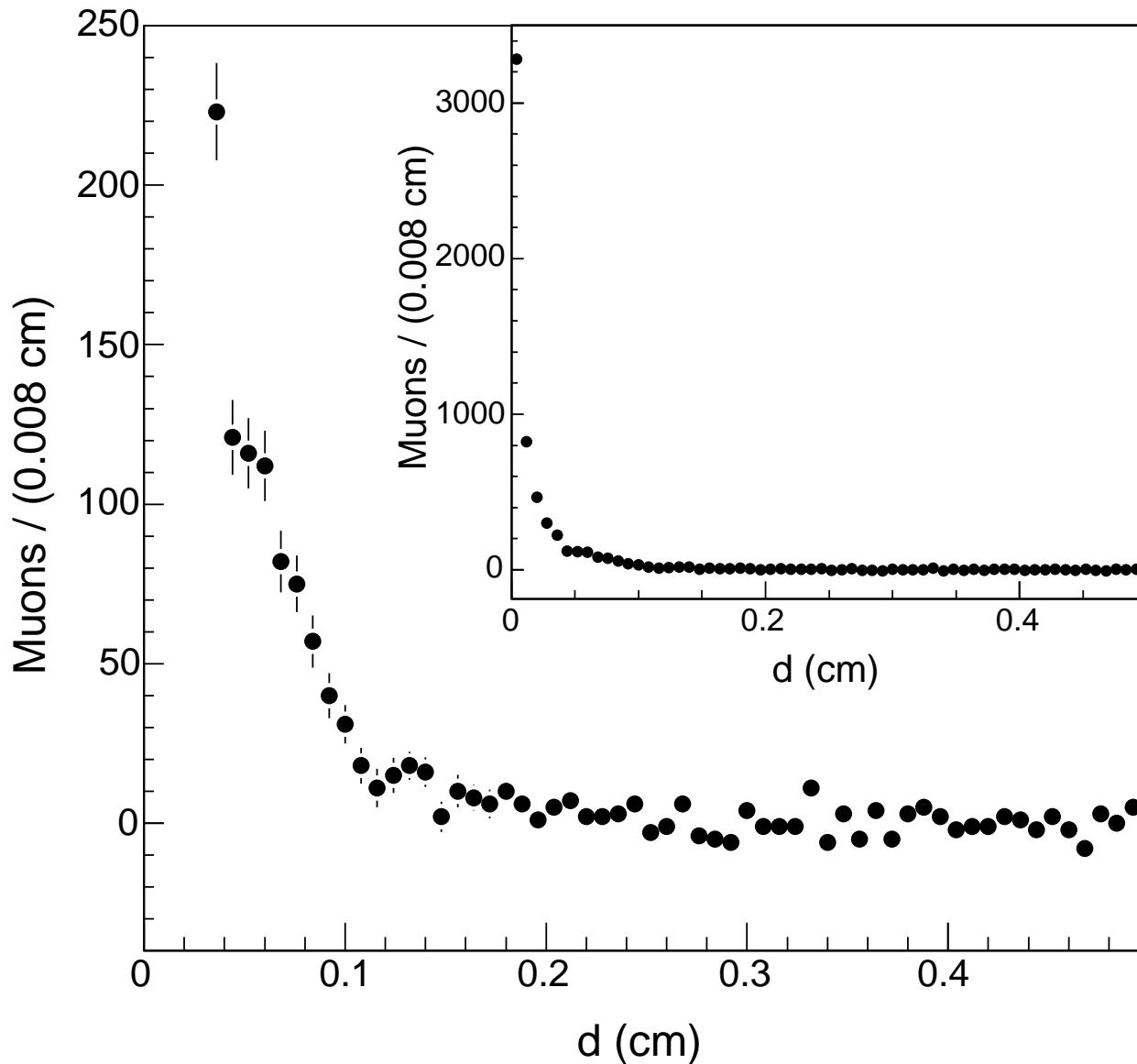


Fig. 6. Magnified impact parameter distribution of additional muons in events in which both trigger muons satisfy the tight SVX selection. The fake muon contribution has been subtracted. The entire distribution is shown in the insert. Additional muons are selected without any SVX requirements.

des Particules/CNRS; the Russian Foundation for Basic Research; the Ministerio de Ciencia e Innovación, Spain; the European Community's Human Potential Programme; the Slovak R&D Agency; and the Academy of Finland.

References

1. T. Aaltonen *et al.*, ArXiv:0810.5357.
2. F. Happacher *et al.*, Phys. Rev. D **73**, 014026 (2006); F. Happacher, *Status of the Observed and Predicted $b\bar{b}$ Cross Section at the Tevatron*, Proceedings of Tsukuba 2006, Deep inelastic scattering, edited by M. Kuze, K. Nagano, K. Tokushuku, World Scientific, 645 (2007).
3. G. Apollinari *et al.*, Phys. Rev. D **72**, 072002 (2005).

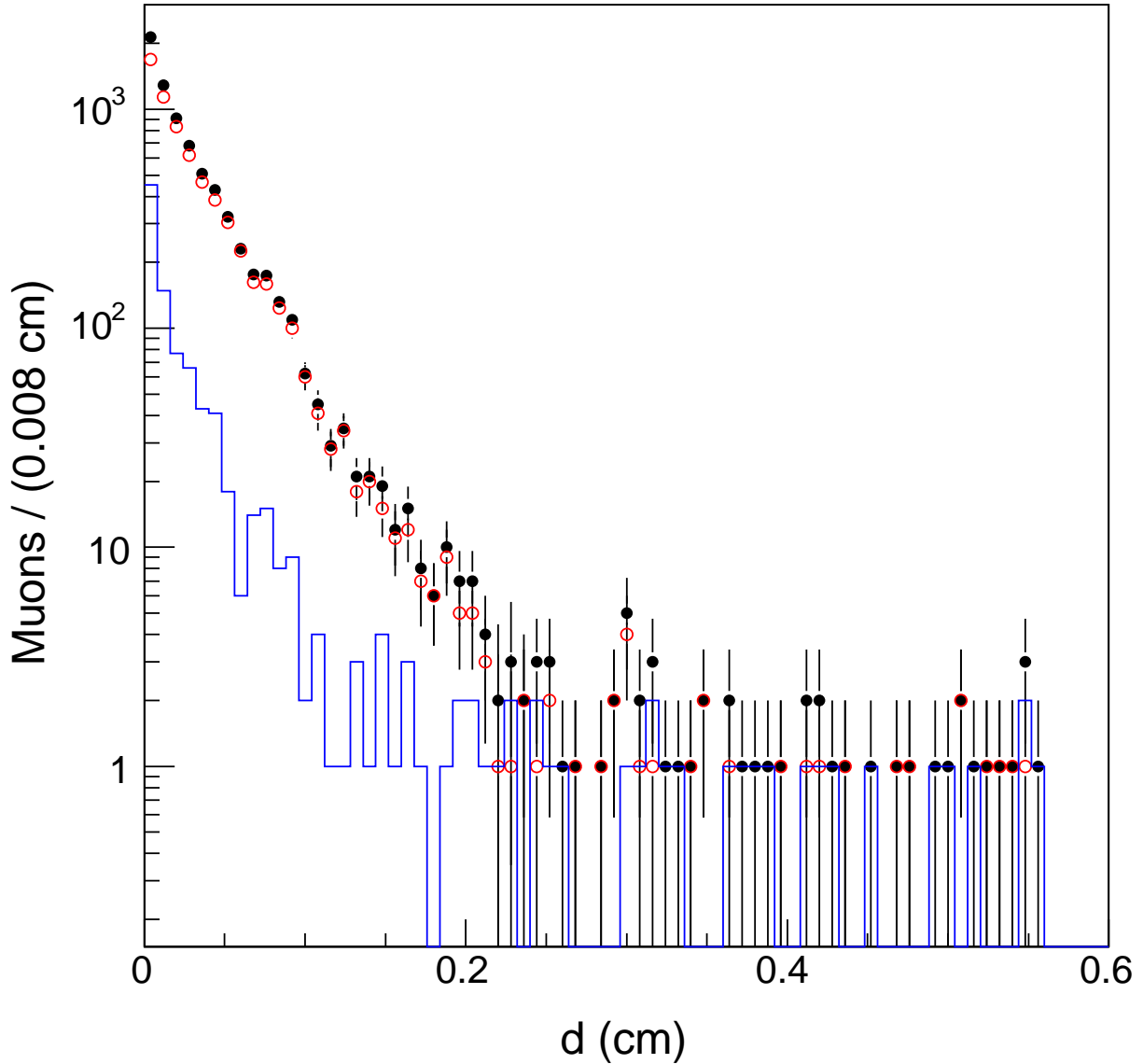


Fig. 7. Impact parameter distributions of muons accompanied by a D^0 candidate and selected as the additional muons in this analysis. No SVX requirements are applied. All events (\bullet) are split into right-sign $\mu^- K^- \pi^+$ (\circ) and wrong-sign $\mu^+ K^- \pi^+$ (histogram) combinations [18]. Muons in wrong-sign combinations are fake. The contribution of the combinatorial background under the D^0 signal has been removed with a sideband subtraction method [1]. The integral of these distributions above 0.35 cm is zero.

4. D. Acosta *et al.*, Phys. Rev. D **69**, 012002 (2004).
5. W.-M. Yao *et al.*, J. Phys. G **33**, 1 (2006).
6. T. Aaltonen *et al.*, Phys. Rev. D **77**, 072004 (2008).
7. D. Acosta *et al.*, Phys. Rev. D **71**, 032001 (2005); R. Blair *et al.*, Fermilab Report No. FERMILAB-Pub-96/390-E (1996); C. S. Hill *et al.*, Nucl. Instrum. Methods Phys. Res., Sect. A **530**, 1 (2004); S. Cabrera *et al.*, Nucl. Instrum. Methods Phys. Res., Sect. A **494**, 416 (2002); W. Ashmanskas *et al.*, Nucl. Instrum. Methods Phys. Res., Sect. A **518**, 532 (2004).
8. The impact parameter is defined as the distance of closest approach of a track to the primary event vertex in the transverse plane with respect to the beamline.

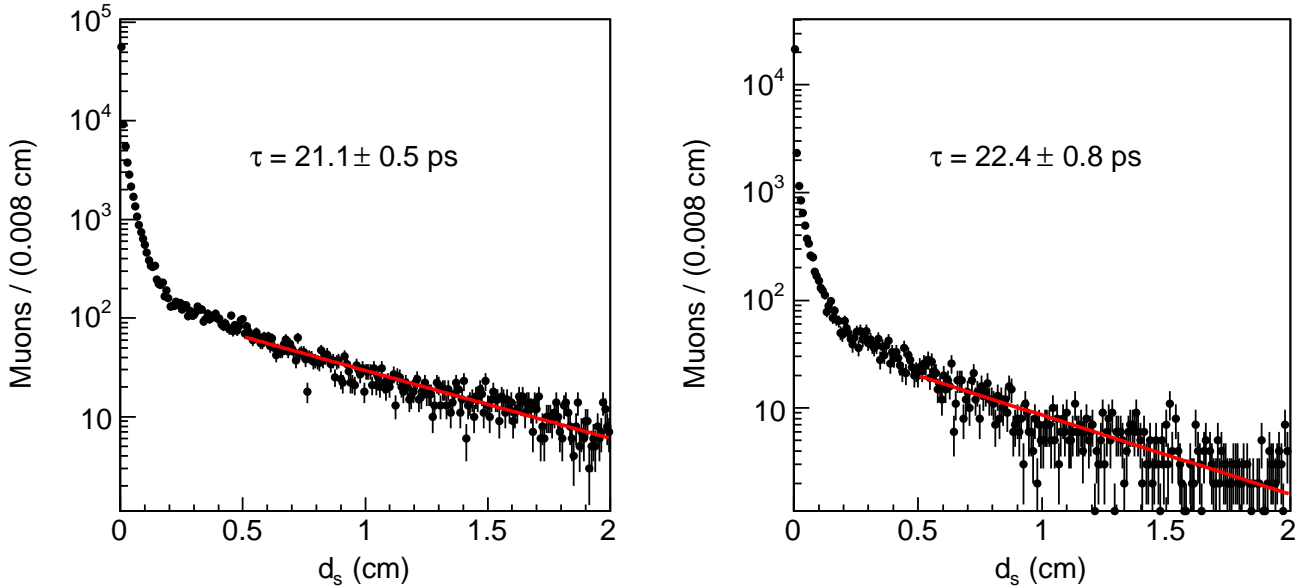


Fig. 8. Impact parameter (d_s) distributions of additional muons for events containing (a) only two muons or (b) more than two muons in a $\cos\theta \geq 0.8$ cone. The solid lines represent fits to the data distributions with an exponential function.

9. We follow the methodology pioneered by previous measurements that ignored other possible sources of muons. For example, muon tracks from pion and kaon in-flight-decays inside the tracking volume were regarded as prompt tracks because the track reconstruction algorithms were believed to remove decay muons with an appreciable kink.
10. D. Acosta *et al.*, Phys. Rev. D **69**, 072004 (2004).
11. T. Shears, *Charm and Beauty Production at the Tevatron*, Proceedings of the Int. Europhys. Conf. on High Energy Phys., PoS (HEP2005), 072 (2005).
12. F. Abe *et al.*, Phys. Rev. D **55**, 2546 (1997).
13. B. Abbott *et al.*, Phys. Lett. B **487**, 264 (2000).
14. This procedure assumes that ghost events are completely rejected by the tight SVX requirements.
15. The 742 pb^{-1} subsample is chosen for direct comparison to the recent CDF $b\bar{b}$ cross section measurement.
16. T. Affolder *et al.*, Phys. Rev. D **64**, 032002 (2001); Erratum-ibid. **67**, 119901 (2003).
17. A correlation factor as large as 0.5 is expected if initial and additional muons are produced in the decay of long-lived particles or by secondary interactions in the detector volume.
18. We reconstruct D^0 candidates by attributing the kaon mass to the track with the same charge as the muon (RS combinations as expected for $\mu^- + D^0$ systems produced by B decays). Wrong-sign (WS) combinations are a measure of the fake muon contribution.